DOI: 10.1002/ejoc.200801184

Synthesis of *exo*-3-Amino-7-azabicyclo[2.2.1]heptanes as a Class of Malarial Aspartic Protease Inhibitors: Exploration of Two Binding Pockets

Martina Zürcher,[a] Fraser Hof,[b] Luzi Barandun,[a] Andri Schütz,[a] W. Bernd Schweizer,[a] Solange Meyer,[c] Daniel Bur,[c] and François Diederich*[a]

Dedicated to Professor Alain Krief

Keywords: Malaria / Plasmepsins / Molecular recognition / Inhibitors / Nitrogen heterocycles

The increasing prevalence of drug-resistant strains of malaria-causing *Plasmodium* parasites necessitates the development of therapeutic agents that inhibit new biochemical targets. We herein describe the design, synthesis, and in vitro evaluation of a class of inhibitors that target the malarial aspartic proteases known as the plasmepsins. The title compounds feature a 7-azanorbornane skeleton that bears an *exo*-amino function, which was designed to interact with the catalytic dyad of aspartic proteases while providing vectors for the attachment of binding elements that target the flap and S1/S3 binding pockets at the enzyme active site. Their synthesis takes advantage of a solvent-free and highly diastereoselective conjugate addition of amines to bicyclic vinyl sulfones. Structural optimization based on a little-known conformational preference of aryl sulfones produced the most potent inhibitors of this new class. In vitro assays demonstrate that the title compounds are capable of potent ($IC_{50} \geq 10$ nM) inhibition of plasmepsins, while remaining relatively weak inhibitors of the closely related human enzymes cathepsins D and E. The ideal occupation of the flap pocket is crucial for both potency and selectivity over the human proteases. Differently functionalized compounds were synthesized to gain new insights into the molecular recognition properties of this cavity.

Introduction

With up to 600 million infections annually, malaria remains a major worldwide health issue.[1] Recent decades have witnessed the increasing prevalence of drug-resistant *Plasmodium* parasites that threaten to render current treatments obsolete.[2] In the search for new therapies with novel modes of action, attention has turned to the consumption of hemoglobin as a source of amino acids for growth and development of the parasites. Blocking the vacuolar digestive enzymes that mediate the degradation of human hemoglobin is a potential approach to antimalarial chemotherapy.[3,4] In *P. falciparum*, the most dangerous of the four human-infecting *Plasmodium* species, three aspartic proteases [plasmepsins (PMs) I, II, and IV] and a histo-aspartic protease (HAP, formerly PM III) have been characterized.[5] These four enzymes have been implicated in the initial steps of the hemoglobin degradation process, and their inhibition with an aspartic protease inhibitor results in the death of the parasite in vitro.[6] The four proteases display mutually redundant activity, suggesting that the inhibition of all four is required to completely block parasite activity.[7,8] It has even been called into question whether the PMs are viable drug targets.[8–10] They are, however, still thought to play a key role, even if the exact nature of their function is not yet clear: Based on knock-out studies, it was suggested that the PMs have crucial roles in the vacuole that also affect other functions.[11] Other recent studies suggest that these aspartic proteases are activated by the malarial cysteine proteases, the falcipains.[12] The design of new inhibitors for these malarial enzymes therefore not only serves to validate general molecular recognition principles; it ultimately also aims to further elucidate the exact roles of the PMs.

Among the four target enzymes, only the structure of PM II has been extensively characterized. In complex with several peptidomimetic inhibitors, the protease adopts a classic pepsin-like fold.[3,13] In three published structures of

[a] Laboratorium für Organische Chemie, ETH Zürich, Hönggerberg HCI
Wolfgang-Pauli-Strasse 10, 8093 Zürich, Switzerland
Fax: +41-44-632-1109
E-mail: diederich@org.chem.ethz.ch
Homepage: http://www.diederich.chem.ethz.ch
[b] Department of Chemistry, University of Victoria
Victoria, BC, V8W 3V6, Canada
[c] Drug Discovery, Chemistry & Biology, Actelion Pharmaceuticals Ltd
Hegenheimermattweg 91, 4123 Allschwil, Switzerland
Supporting information for this article is available on the WWW under http://www.eurjoc.org/ or from the author.

PM II in complex with small-molecule, nonpeptidic inhibitors, a new binding pocket (the flap pocket) has been exposed by a major conformational reorganization.[14,15] The existence of this cavity had previously been proposed on the basis of the homology between PM II and human renin.[16] Our early efforts at the structure-based design of inhibitors that target the flap pocket of PM II produced functionalized bicyclic amines that displayed IC_{50} values (concentration at which 50% maximal initial velocity is observed) of 3–35 μM (Figure 1a).[16–18] Aided by the first available X-ray crystal structure of PM II in the flap-open conformation,[14] we later optimized these compounds and reported a second generation of bicyclic inhibitors featuring a donor-rich *endo*-2-sulfonyl-*exo*-3-amino-7-azabicyclo[2.2.1]heptane core.[19] This "diamine needle" should address the catalytic aspartate dyad as shown in Figure 1b and thereby anchor the inhibitor in a preferred conformation. The aspartic acids Asp34 and Asp214 adopt a variety of protonation states, depending on the identity of their binding partner and the environmental pH.[20,21]

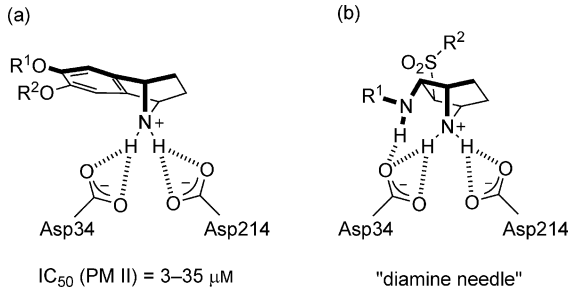

Figure 1. Proposed interaction of (a) our first-generation inhibitors[16–18] and (b) the new *exo*-3-amino-7-azabicyclo[2.2.1]heptane inhibitors.[19] The (protonated) azanorbornane (referred to as "diamine needle") addresses the catalytic Asp dyad, R^1 targets the S1/S3 site, and R^2 occupies the flap pocket of PM II. The earlier benzannellated azanorbornane needles, bound to the catalytic dyad, feature unfavorable secondary electrostatic repulsions between the Asp side chains and the electron-rich π system, whereas the new needles engage with the *exo*-amine moiety via an additional, and favorable, H-bond interaction.

After thorough conformational analysis and modeling, these compounds were designed such that the *exo*-N atom directs an appended substituent R^1 to the S1/S3 pocket, while simultaneously donating an additional H bond to the catalytic dyad (Figure 1b).[19,22] The *endo*-sulfone substituent should target the flap pocket with a vector R^2. Calculations[19,23] as well as a recent survey of the Cambridge Structural Database (CSD)[24] demonstrated that aryl sulfones strongly prefer a geometry in which the π orbitals of the aryl ring bisect the sulfone O atoms (i.e., θ = 90°, cf. Figure 2). This relatively rigid geometry should help to position the vector R^2 such that it is nicely directed into the flap pocket. In addition, the sulfone function serves to attenuate the basicity of the amines. The conformational preferences of aryl sulfones resembles the one observed for sulfonamides[25] and methylsulfonyl methyl carbanions[26] and can be explained by stereoelectronic effects: the p orbital at C2 (see Figure 2) interacts with the lowest-lying σ* orbital (p→σ*) of the weakest bond, which is the S–C1 bond.

The first resulting inhibitors display IC_{50} values as low as 45 nM against PM II. Importantly, these compounds are also potent inhibitors of PM I ($IC_{50} \geq 100$ nM) and IV ($IC_{50} \geq 10$ nM) and display good selectivity over the closely related human enzymes cathepsins D and E (hCat D and E).[19] The latter proteases degrade dysfunctional hemoglobin and must not be inhibited. These results validate PM II as a model for all PMs for this class of inhibitors, which is particularly important in the absence of cocrystal structures of the other target enzymes in the flap-open conformation. Compound (±)-**1**, which lacks a vector directed into the flap pocket, shows dramatically reduced activity relative to that of (±)-**2** or (±)-**3** (Figure 3). Chiral resolution of (±)-**3** further confirmed the proposed binding mode: the resulting

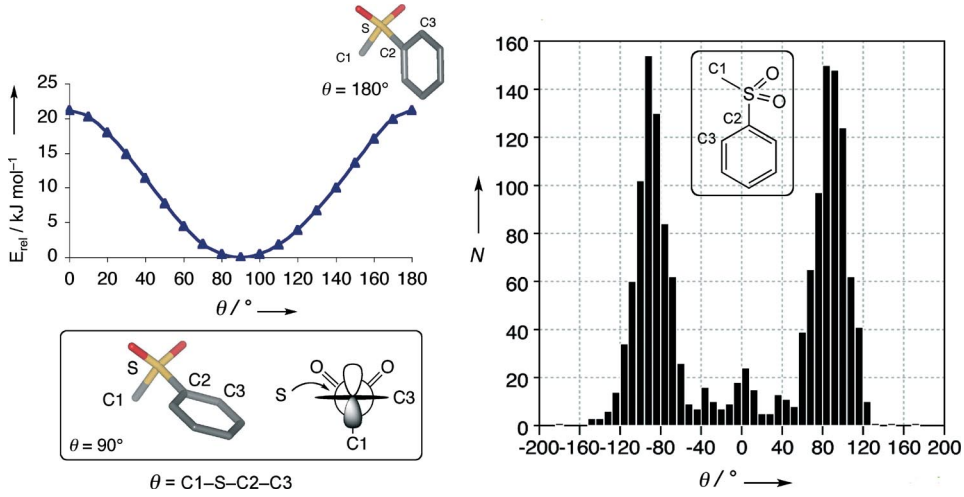

Figure 2. Conformational preferences of aryl sulfones. Left: The C_{aryl}–S bond of phenyl methyl sulfone was driven through all possible dihedral angles θ. The lowest energy conformation (θ = 90°) is shown in two representations in the box. DFT-B3LYP calculations were carried out by using the 6-31G* basis set and MP2 correlation. Right: Histogram of dihedral angle occurrences in the CSD confirming the preference of the pictured sulfone fragment for θ = 90°.[24]

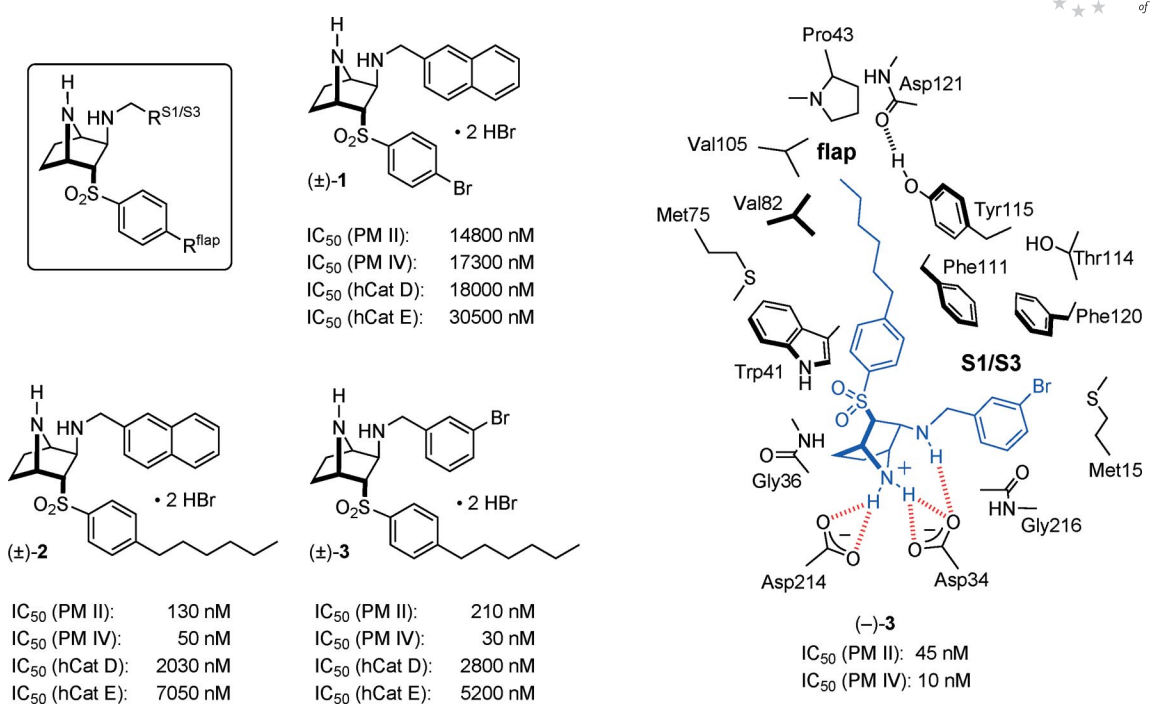

Figure 3. Left: General structure of the inhibitors featuring a "diamine needle" (box) and three examples. Right: Proposed binding mode of the active enantiomer (–)-**3**.

inhibitors (+)-**3** and (–)-**3** displayed activities that differ by as much as 3000-fold [IC_{50} (PM II) = 3260 and 45 nM, respectively; IC_{50} (PM IV) = 33900 and 10 nM, respectively]. This result, taken together with a careful modeling study of each enantiomer within the active site of PM II, suggests that the structure of (–)-**3** be assigned as the 2*S*,3*R* enantiomer, pictured in Figure 3 (right).[19,22] These findings indicate that binding within the flap pocket is important and prompted us to investigate this cavity more closely. Alcohols, alkynols, ethers, and fluorinated compounds were prepared to further optimize binding and elucidate the recognition properties of this extremely important pocket. In parallel, the S1/S3 vector was also optimized, while maintaining the powerful "diamine needle" motif.

Results and Discussion

A flexible synthesis was developed to generate derivatives with a variety of S1/S3 and flap vectors. We hypothesized that the substituent that targets the S1/S3 pocket could be introduced by conjugate addition of amines to the vinyl sulfone (±)-**4** (Scheme 1). The aryl bromide function would on the other hand allow introduction of various flap vectors via different cross-coupling reaction methods. The synthesis of (±)-**4** is outlined in Scheme 1: 4-Bromobenzenesulfonyl chloride (**5**) undergoes a Friedel–Crafts-type reaction with bis(trimethylsilyl)acetylene (**6**), and SiO_2-mediated deprotection[27] leads to the aryl alkynyl sulfone **7** in 30% yield. The Diels–Alder reaction of this intermediate with *N*-Boc-pyrrole (Boc = *tert*-butyloxycarbonyl) provides the bicyclic diene (±)-**8** (75%), and subsequent selective reduction of the more electron rich double bond by using in situ prepared "Ni_2B"[28] proceeds smoothly to give vinyl sulfone (±)-**4** (100%).

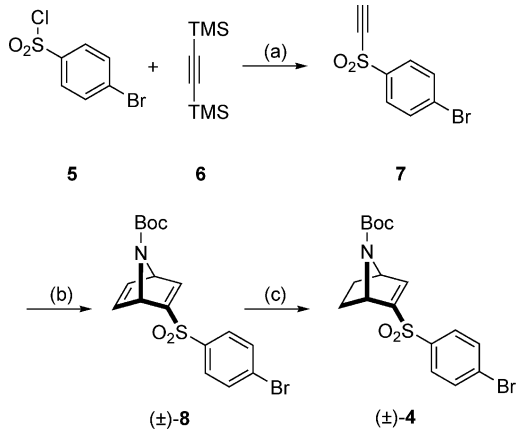

Scheme 1. (a) 1. $AlCl_3$, CH_2Cl_2, 0 °C → 25 °C, 18 h; 2. SiO_2; 30%. (b) *N*-Boc-pyrrole, 80 °C, 18 h; 75%. (c) $[Ni(OAc)_2(H_2O)_4]$, $NaBH_4$, EtOH, THF, HCl, 25 °C, 16 h; 100%.

Introduction of the S1/S3 Vector

The conjugate addition was achieved by heating vinyl sulfone (±)-**4** with an alkylamine at 70–90 °C in the absence of solvent (Scheme 2). Especially on small scale, the yields could be improved by premixing two solid reagents in a minimal amount of CH_2Cl_2, followed by evaporation of the solvent, before heating.

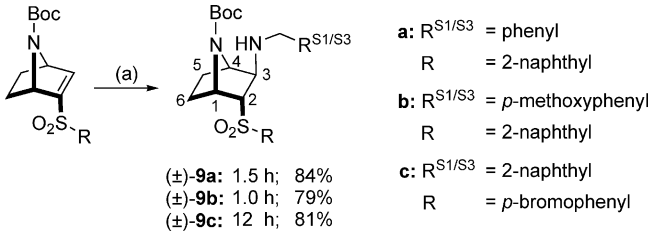

Scheme 2. (a) Alkylamine, 70–90 °C. A variety of alkylamines are tolerated, see the Supporting Information for experimental details.

Although this reaction can generate four possible diastereoisomeric products, in every case the desired *endo*-2-sulfonyl-*exo*-3-amino diastereoisomer is the major isomer produced (19:1 to 170:1 diastereoisomeric ratio) and is isolated in good yields (for examples, see Scheme 2). The identity of the major diastereoisomer was first proposed on the basis of 2D-NMR spectroscopic studies of compound (±)-**9a** (Figure 4a) and later confirmed by the X-ray crystal structure of (±)-**9b** (Figure 4b). In addition, the absence of ^3J coupling between bridgehead protons (H_{bh}) and *endo* protons (H_{endo}), due to a rigidly fixed mutual dihedral angle θ of 90° (Figure 4c), provides a simple 1D-NMR spectroscopic probe into the identity of all 2,3-disubstituted 7-azabicyclo[2.2.1]heptanes subsequently described in this paper.

The selective production of the *endo*-2-sulfonyl-*exo*-3-amino isomer of (±)-**9** can be attributed to the ability of the 7-azabicyclo[2.2.1]heptane core to direct incoming reagents to its *exo* face.[17,29,30] After conjugate addition of the amine to the *exo* face of C3, the intermediate sulfonyl-stabilized carbanion likely equilibrates to provide the *endo*-sulfone at C2, an arrangement that minimizes steric repulsion with the neighboring amino substituent (for numbering of the azanorbornane scaffold, see Scheme 2).

Variation of the Flap Substituent

With intermediate (±)-**9c** in hand, the way was paved for the variation of the flap vector. With the 2-methylnaphthyl moiety left constant as the S1/S3 substituent, various residues could be attached to the aryl bromide via cross-coupling reactions (Scheme 3): A Suzuki reaction of (±)-**9c** with hexylboronic acid, using the method of Buchwald and coworkers,[31] gave (±)-**10** in 65% yield, and subsequent treatment with BBr_3 at –78 °C quantitatively yielded the product (±)-**2** as the bis(hydrobromide) salt. Aryl bromide (±)-**9c** was also elaborated by using Sonogashira coupling reactions with different alk(en)ynes **11a**–**q** to furnish the unsaturated compounds (±)-**12a**–**q**. Hydrogenation with the use of Adams' catalyst[32] gave the alkanes (±)-**13a**–**q**, and deprotection with either BBr_3 at –78 °C or sequential treatment with *tert*-butyldimethylsilyl trifluoromethanesulfonate (TBSOTf) in CH_2Cl_2 and CsF/HOAc in DMF[33] yielded the products (±)-**14a**–**q** (42–100%). The bromide (±)-**9c** was also quantitatively deprotected to give compound (±)-**1**, lacking the flap-vector chain. Through a Heck reaction, vinyl ether (±)-**15** was available from (±)-**9c** and could be converted into (±)-**16** via (±)-**17** by the described methodology.

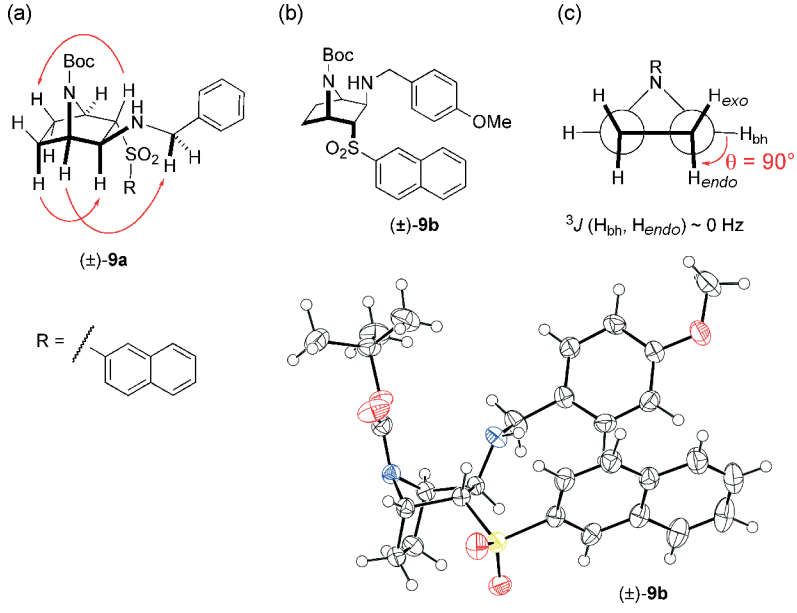

Figure 4. Identification of the major diastereoisomers produced by the conjugate addition of alkylamines to vinyl sulfones of type (±)-**4**. (a) 2D-NOE correlations observed for compound (±)-**9a**. (b) Structure of (±)-**9b** determined by X-ray diffraction (see Experimental Section). (c) Newman projection illustrating that in the 7-azabicyclo[2.2.1]heptane ring system, bridgehead protons (H_{bh}) couple exclusively with *exo*-protons (H_{exo}), while a 90° dihedral angle θ produces zero coupling between H_{bh} and H_{endo}. The resultant characteristic splitting pattern allows 1D-^{1}H-NMR spectroscopic identification of the *endo*-2-sulfonyl-*exo*-3-amino isomers in every case.

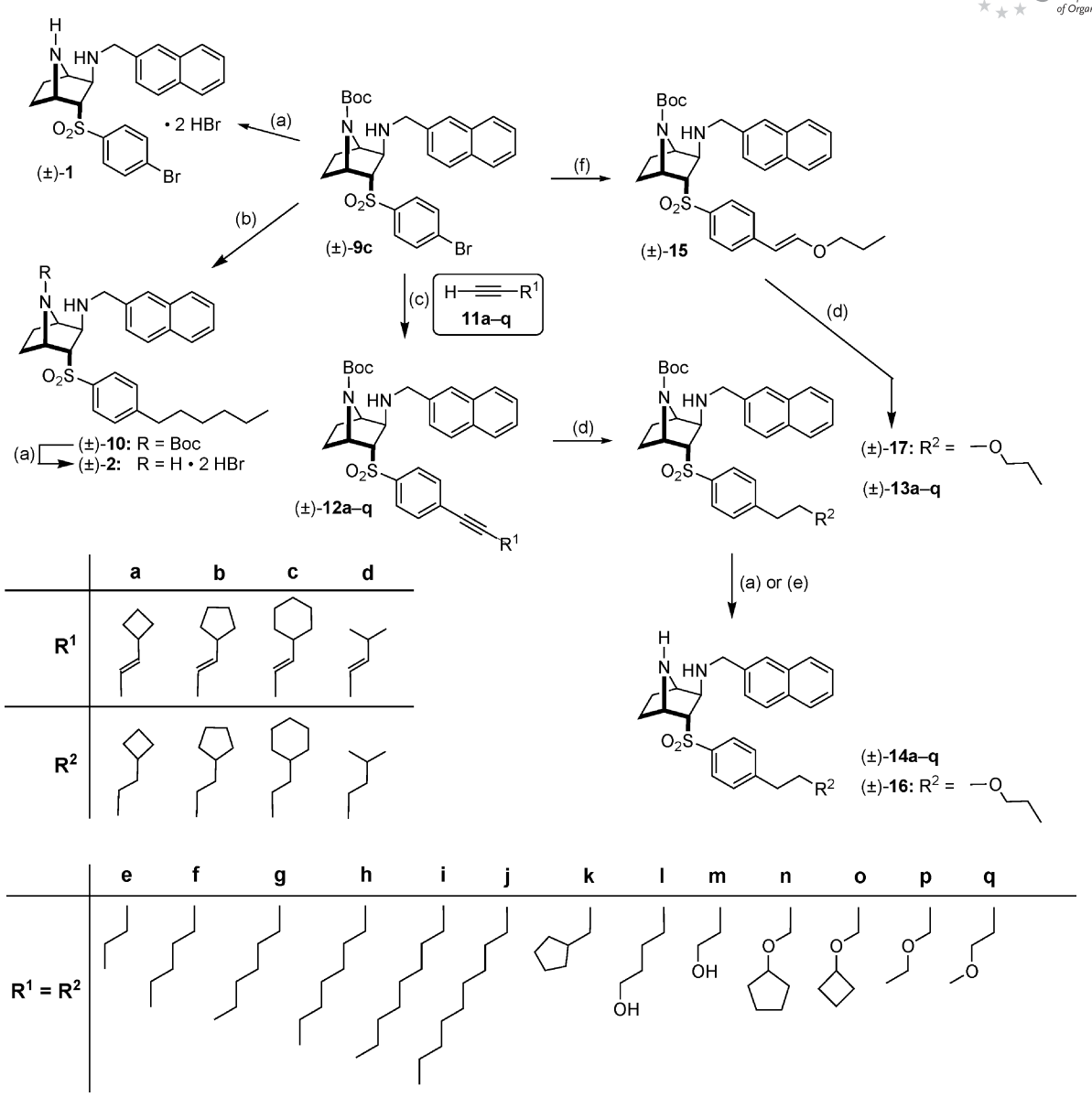

Scheme 3. (a) BBr_3, CH_2Cl_2, –78 °C, 15 min; 85–100%. (b) $C_6H_{13}B(OH)_2$, $Pd(OAc)_2$, 2-(dicyclohexylphosphanyl)biphenyl, K_3PO_4, toluene, 80 °C, 16 h; 65%. (c) One of the alk(en)ynes (±)-**11**–**q**, CuI, $[PdCl_2(PPh_3)_2]$, $HNEt_2$, 55 °C, 11–18 h; 50–93%. (d) H_2, PtO_2, EtOH, 25 °C, 8–17 h; 50–100%. (e) TBSOTf, 2,6-lutidine, CH_2Cl_2, 25 °C, 30 min; then HOAc, CsF, DMF, 25 °C, 30 min; then HCl, EtOH; 42–99%. (f) Propyl vinyl ether, NEt_3, $Pd(OAc)_2$, PPh_3, 80 °C, 95 h; 59%.

Phenol ether (±)-**18** was synthesized as outlined in Scheme 4. A Williamson ether synthesis starting from phenol and 1-bromopentane gave ether **19**, which was converted into sulfonyl chloride **20**. In analogy to the synthesis described for intermediate (±)-**9c**, and after deprotection with BBr_3, (±)-**18** was obtained in good yield.

The alcohols (±)-**13l** and (±)-**13m** were converted into (±)-**21a** and (±)-**21b** by nucleophilic fluorination by using (diethylamino)sulfur trifluoride (DAST) (Scheme 5).[34] Surprisingly, the attempted deprotection of (±)-**21a** with BBr_3 led to a Finkelstein reaction, and only impure (±)-**22** could be isolated. The alternative conditions described above, using TBSOTf, however, gave access to the desired fluorinated inhibitors (±)-**23a** and (±)-**23b**.

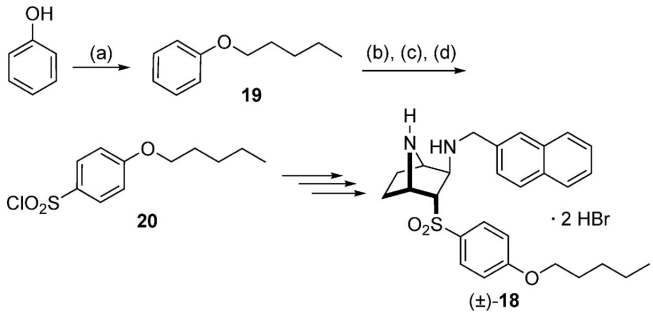

Scheme 4. Synthesis of phenol ether (±)-**18**. (a) K_2CO_3, 1-bromopentane, acetone, 65 °C, 1 h; 70%. (b) $ClSO_3H$, 1,2-dichloroethane, 12 h. (c) NaCl, H_2O. (d) $POCl_3$, 170 °C, 1.5 h; then 1,2-dichloroethane, 95 °C, 1 h; 57% (over 3 steps).

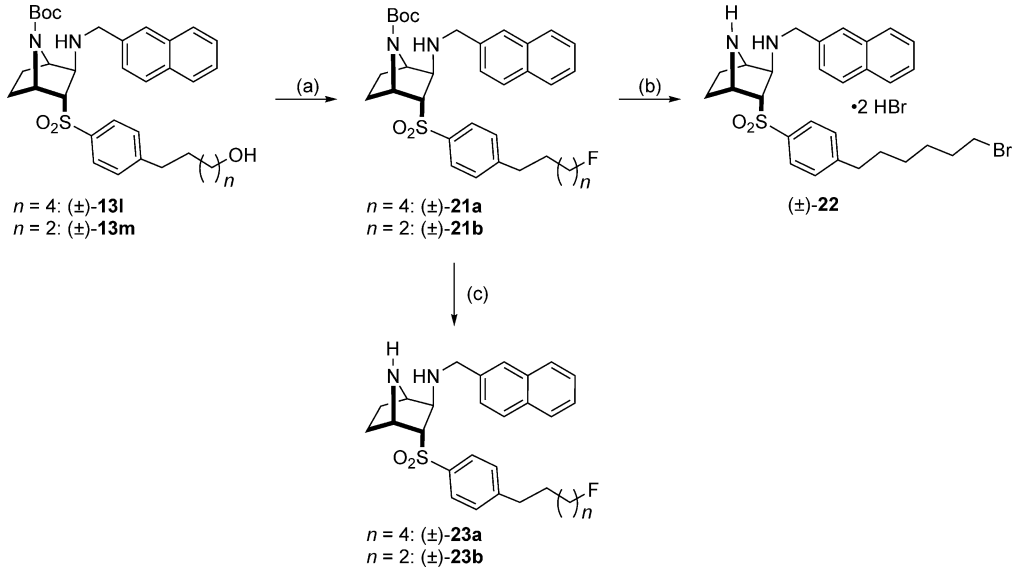

Scheme 5. (a) DAST, CH_2Cl_2, –78 °C → 25 °C, 20 h; 50% (n = 2) and 55% (n = 4). (b) BBr_3, CH_2Cl_2, –78 °C, 15 min; impure. (c) TBSOTf, 2,3-lutidine, CH_2Cl_2, 25 °C, 30 min; then K_2CO_3, THF/MeOH, 25 °C, 1 h; 54% (n = 2) and 30% (n = 4).

Variation of the S1/S3 Substituent

Inhibitors (±)-**3** and (±)-**24**–(±)-**28** were synthesized to explore the binding of biaryls within the S1/S3 pocket (Scheme 6). 4-Hexylbenzenesulfonyl chloride was converted into vinyl sulfone (±)-**29** by using the familiar methodology outlined in Scheme 1 (see the Supporting Information for experimental details). Conjugate reaction with 3-bromobenzylamine at 70 °C gave the desired diastereoisomer (±)-**30** in 65% yield. Suzuki cross-coupling with a variety of aryl boronic acids furnished compounds (±)-**31a**–**c** in 58–76% yield. Treatment with BBr_3 at –78 °C for 15 min effected selective removal of the Boc groups to give inhibitors (±)-**24**, (±)-**25**, and (±)-**27**, while treatment with BBr_3 at 25 °C for 3 h additionally removed the methyl ethers to provide compounds (±)-**26** and (±)-**28**. Intermediate (±)-**30** was similarly deprotected to the aryl bromide-functionalized inhibitor (±)-**3**.

Biochemical Evaluation and Interpretation

All synthesized compounds were evaluated for their in vitro activity against PM II by using a fluorescence-based

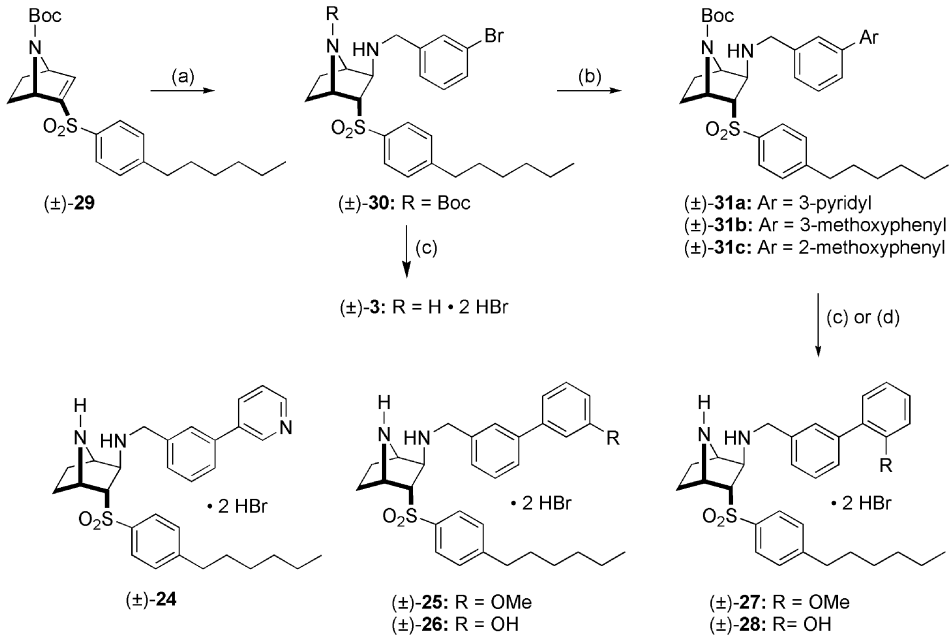

Scheme 6. (a) 3-Bromobenzylamine, 70 °C, 1 h; 65%. (b) $ArB(OH)_2$, $Pd(OAc)_2$, 2-(dicyclohexylphosphanyl)biphenyl, K_3PO_4, DMF, 90 °C, 16 h; 58–76%. (c) BBr_3, CH_2Cl_2, –78 °C, 15 min; 100%. (d) BBr_3, CH_2Cl_2, –78 → 25 °C, 3 h; 100%.

proteolysis assay.[14] Exemplary compounds were also tested for in vitro inhibition of PM I and IV or for their activity against hCat D and E. The results, including the previously reported activities of (±)-**1**, (±)-**2**, (±)-**3**, (±)-**27**, and (±)-**28**,[19] as well as (±)-**14e**, (±)-**14f**, and (±)-**32**[35] are summarized in Tables 1–3.

Generally, the described inhibitors display submicromolar activity against the three PMs, while remaining poorly active against the closely related human enzymes. The exceptions to this statement are instructive. Compound (±)-**1**, which lacks the *n*-hexyl chain directed into the flap pocket, shows dramatically reduced activity relative to all other reported inhibitors (Table 1). This indicates that binding within the flap pocket is (a) energetically important and (b) accessible for all three PMs studied. It additionally suggests that the flap pocket of hCat D and E is either structurally dissimilar or lacking altogether.

Table 1. IC_{50} values of some of the discussed "diamine needle" inhibitors.

	IC_{50}[a] / nM				
	PM I[b]	PM II[c]	PM IV[c]	hCat D[c]	hCat E[c]
(±)-**1**	n.d.	14800	17300	18000	30500
(±)-**2**	100	130	50	2030	7050
(±)-**3**	150	210	30	2800	5200
(±)-**14n**	n.d.	820	620	13200	42200
(±)-**14o**	n.d.	1990	1440	14350	39340
(±)-**14p**	n.d.	6860	3640	17300	33000
(±)-**24**	n.d.	820	260	4250	14350
(±)-**25**	n.d.	520	170	2210	8700
(±)-**26**	n.d.	400	180	1440	5140
(±)-**27**	210	390	180	1410	5910
(±)-**28**	290	400	110	1500	5400

[a] IC_{50} values are averages of 2–3 repetitions of a fluorescence-based proteolysis assay.[14,36] [b] Values determined at Washington University as previously reported:[36] [enzyme] = 1 nM, [substrate] = 1 mM, 100 mM acetate buffer, pH 5.1. [c] Values determined at Actelion Pharmaceuticals: [enzyme] = 1 nM, [substrate] = 1 mM, 50 mM acetate buffer, pH 5.0, 12.5% glycerol, 10% DMSO, 0.1% bovine serum albumin. Measurements at 37 °C. n.d. = not determined.

Another interesting observation arises when comparing the activities of inhibitors (±)-**2** [IC_{50}(PM II) = 130 nM] and (±)-**14p** [IC_{50}(PM II) = 6860 nM], which differ only by a single $–CH_2–$ to –O– mutation. The presence of the ether O atom within the flap pocket disfavors binding, but the more hydrophobic cyclobutyloxy- and cyclopentyloxy-substituted inhibitors [(±)-**14o** and (±)-**14n**] rescue much of the lost binding energy [IC_{50}(PM II) = 1990 and 820 nM, respectively]. This allows the assumption that the flap pocket tolerates substituents more voluminous than *n*-alkanes and that further optimized compounds will display increased potency. However, as already communicated, oversized substituents reduce activity.[35] Substituted [(±)-**14a**–**d** and (±)-**14k**] and *n*-alkanes (C_4 to C_{11}) occupy the flap pocket with an optimal volume occupancy of ca. 55–60% assuming a constant pocket volume.[35]

To explore the binding preferences of the aryl-favoring[37] S1/S3 pocket, the naphthyl substituent of (±)-**2** was mutated to a variety of biaryl substituents and in one case to a truncated bromoaryl substituent. The biaryl inhibitors (±)-**24**–(±)-**28** displayed equal or slightly reduced activity against PM II and PM IV relative to (±)-**2**, with IC_{50} values between 110 and 820 nM. Most notable was the decreased selectivity for these compounds over hCat D and E. Whereas (±)-**2** displayed a selectivity [IC_{50}(hCat D)/IC_{50}(PM II)] > 15, the biaryl inhibitors (±)-**24**–(±)-**28** displayed IC_{50}(hCat D)/IC_{50}(PM II) < 7. Aryl bromide (±)-**3** is the most potent inhibitor of PM IV among those tested (IC_{50} = 30 nM). In contrast to the larger naphthyl- and biaryl-derived inhibitors, its selectivity factors over the human enzymes are excellent [IC_{50}(hCat D)/IC_{50}(PM IV) ≈ 90; IC_{50}(hCat E)/IC_{50}(PM IV) ≈ 170].

For the large difference in binding of (±)-**2** [IC_{50}(PM II) = 130 nM] and (±)-**14p** [IC_{50}(PM II) = 6860 nM] the following three explanations were considered: (a) conformational effects, (b) energetically unfavorable repulsion between the O lone pairs of (±)-**14p** and the adjacent, electron-rich indole ring of Trp41 (Figure 5), and (c) the energetic penalty associated with desolvating a single ether O atom upon entering a hydrophobic protein cavity. The potential energy surfaces for different conformations of the *n*-hexyl fragment of (±)-**2** and the ethoxypropyl fragment of (±)-**14p**, as evaluated by semiempirical calculations, were relatively smooth.[38] In energy minimizations within the protein, which was held constant, both conformations for (±)-**2** and (±)-**14p**, respectively, were found to be favorable and strain-free.[22] It was therefore concluded that the poor binding of (±)-**14p** can be attributed to some combination of factors (b) and (c).

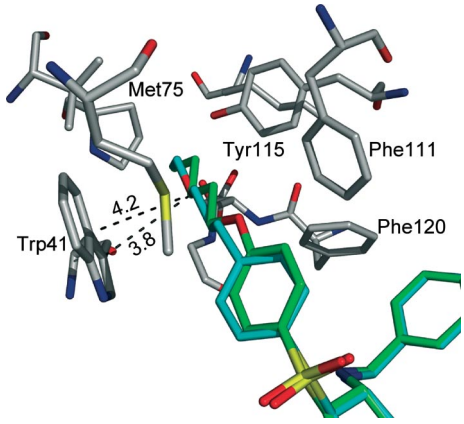

Figure 5. Ethyl ether (±)-**14p** and phenol ether (±)-**18** modeled (MOLOC[22]) in the flap pocket of PM II. Color code: C skeleton of (±)-**14p**: light blue, C skeleton of (±)-**18**: green, C atoms of protein: gray, O atoms: red, N atoms: blue, S atoms: yellow. Distances are given in Å.

To account for the reduced activity of (±)-**14p** relative to that of (±)-**2**, the ethers (±)-**16**, (±)-**18**, and (±)-**14q** were synthesized to see whether the effect was position-dependent or not. Table 2 summarizes the results: Ethyl ether (±)-**14p** shows exceptionally high IC_{50} values for all PMs. The inhibitors with an O atom in the neighboring positions [(±)-**14q** and (±)-**16**] bind better than compound (±)-**14p**, but still show weaker binding than phenol ether (±)-**18** and

Table 2. IC_{50} values for the linear ether series. The *n*-hexyl vector is shown for comparison. Log D values at pH 5.5 and 7.4 were calculated.[39] n.d. = not determined.

	R =	IC_{50}[a] /nM			cLog D at
		PM I	PM II	PM IV	pH 5.5/7.4
	(±)-**2**[c]	100[b]	130	50	3.96/5.68
	(±)-**18**[c]	100	150	60	3.18/4.90
	(±)-**16**[c]	340	900	440	1.84/3.57
(±)	(±)-**14p**[c]	n.d.	6860	3640	1.86/3.59
	(±)-**14q**	360	2190	360	1.54/3.27

[a,b] See footnotes in Table 1. [c] Compounds isolated and tested in the form of their bis(hydrobromide) salts.

lead compound (±)-**2**. Striking is the virtually identical activity of phenol ether (±)-**18** and *n*-hexyl derivative (±)-**2**. Both compounds inhibit PM I, II, and IV quite strongly (IC_{50} values 50–150 nM).

On the one hand, the better activity of (±)-**18** as compared to the other ethers could be explained by the fact that phenol ethers are less solvated than alkyl ethers and the phenolic oxygen atom might be localized at the edge of the pocket. The introduction of an O atom into the *n*-hexyl chain of (±)-**2** does not, in the case of (±)-**18**, substantially decrease the lipophilicity of the compound, as reflected in an only slightly lower cLog D value (Table 2).[39] Thus, the cLog D value for the aryl ether (±)-**18** is significantly higher than for the alkyl ethers, which fits well with the observation that (±)-**18** is apparently introduced more easily into the hydrophobic flap pocket. On the other hand, it should cost a similar amount of energy to desolvate ethers (±)-**14q** and (±)-**16** as compared to (±)-**14p** (again supported by the cLog D values). Energetic differences in desolvation do not appear to be the determining effect, and it is likely that a repulsive interaction between the ether O atom in (±)-**14p** next to the electron-rich π surface of the indole ring of Trp41 determines the overall energy balance (Figure 5). Conformational effects were considered, too. A CSD search confirms that alkyl benzenes and phenol ethers prefer different torsional angles C1–X–C2–C3 (Figure 6). Whereas the four atoms preferentially lay in one plane for phenol ethers (X = O), this is not the case for alkyl substituents (X = CH_2). According to modeling, however, the in-plane conformation is not more favorable at the position, and no repulsions are predicted for either compound.[22]

The effect that the biological activity is lowered upon introduction of an O atom for all ethers except phenol ether (±)-**18** is more pronounced in PM II than in PM I or PM IV. This confirms what was already observed earlier:[35] the flap pockets of PM II and PM IV are not as similar as might be expected based on the overall amino acid sequence homology. Whereas mainly sterics should be determinant for the different optimal lengths of *n*-alkyl vectors,[35] here, electronic effects on intermolecular interactions could be involved as well. Furthermore, it cannot be excluded that certain amino acid side chains in PM II prefer different side chain conformations if compared to PM I and IV.

After these revealing results, the cavity was further explored in terms of its hydrophobicity and hydrophilicity by examining the effects of functional groups such as F and HO. If the terminal CH_3 group of inhibitors (±)-**14f** and (±)-**14e** is replaced by a HO group [(±)-**14l** and (±)-**14m**, Table 3], activity drops markedly. The strength of this effect is different for PM II and PM IV and for different chain

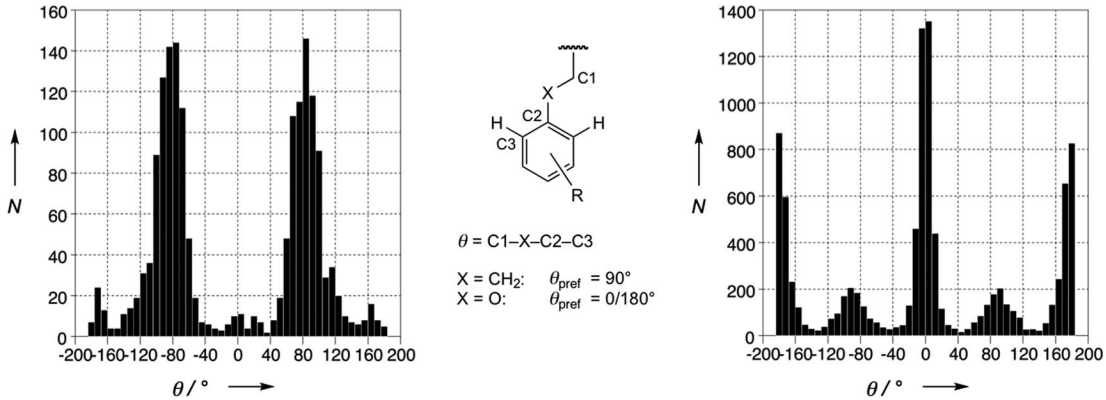

Figure 6. Preferred torsional angles θ_{pref} for (substituted) alkyl benzenes (X = CH_2, left histogram) and phenol ethers (X = O, right histogram) differ as observed in a recent CSD search.[24]

Table 3. IC_{50} values for inhibitors with different heteroatoms in their flap vector. The *n*-alkyl compounds are shown for comparison. Log D values at pH 5.5 and 7.4 were calculated.[39] n.d. = not determined.

	R =	IC_{50}[a] /nM			cLog D at
		PM I	PM II	PM IV	pH 5.5/7.4
(±)-**14f**[c]		n.d.	50	210	4.49/6.22
(±)-**2**		100[b]	130	50	3.96/5.68
(±)-**14e**[c]		n.d.	680	240	3.43/5.16
(±)-**32**		n.d.	4190	1480	2.90/4.62
(±)-**14l**[c]	OH	170	790	640	1.95/3.68
(±)-**14m**[c]	OH	430	4610	6490	1.03/2.76
(±)-**33**	OH	4580	15700	13000	1.68/3.41
(±)-**23a**	F	30	350	80	3.18/4.91
(±)-**23b**	F	980	2210	1920	2.19/3.92

[a,b] See footnotes in Table 1. [c] Compounds isolated and tested in the form of their bis(hydrobromide) salts.

lengths, probably because the desolvated HO group is placed in more or less hydrophobic regions of the enzyme pocket without formation of new intermolecular H bonds. A comparison of (±)-**14l** and (±)-**33** [which was synthesized by deprotection of (±)-**12l**] shows clearly that a rigid, straight alkyne moiety is not well tolerated. This is in agreement with our hypothesis that the flexible alkyl chains can adapt themselves to the pocket,[35] whereas the newly introduced triple bond makes the relatively large vector too rigid to be well accommodated within the cavity. Finally, one H atom of the terminal CH_3 group of (±)-**32** and (±)-**2** was replaced by a F atom to further explore the cavity. The results are not conclusive yet, and a variety of fluorinated derivatives will be prepared for a "fluorine scan"[40,41] to further elucidate the favorable and unfavorable fluorine interactions of the flap pocket.

Importance of the Aryl Sulfone Function

As explained in the Introduction, the aryl sulfone moiety was chosen to guarantee a relatively rigid geometry, properly preorganized for binding, and it should also attenuate the basicity of the two amine centers in the "diamine needle" anchor. Two X-ray crystal structures of Boc-protected inhibitor precursors could be obtained. The torsional angles C1–S–C2–C3 (cf. Figure 2) are 107° [(±)-**9b**] and 101° [(±)-**13f**], which is in good agreement with the conformational preferences seen for aryl sulfones in calculations and a CSD search (see above).

Exemplary ligands were subjected to experimental pK_a measurements (Table 4). The measured pK_a values are indeed markedly lower than normally expected for secondary amines (e.g., pyrrolidine in water: pK_a = 11.31, dimethylamine: pK_a = 10.8).[42–44] The pK_a value of unsubstituted 7-azanorbornane has been measured as 10.8.[45] In our ligands, the experimental first pK_a value is around 6.3. Under the conditions of the biological assay (pH 5), only one amine center is protonated, as the second pK_a value is measured around ≈3 (Table 4).

Table 4. Results of the pH-metric determination of pK_a values[a] for exemplary compounds.

	pK_{a1}	pK_{a2}
(±)-**14d**	3.1	6.2
(±)-**14k**	3.1	6.1
(±)-**18**	3.4	6.4
(±)-**23a**	2.8	6.3
(±)-**23b**	2.9	6.3

[a] pK_a values were determined with a potentiometric titration method in 0.15 M KCl aqueous solution at 25 °C. Because of the low solubility of the compounds above pH 7, methanol (63% v/v) was used as a cosolvent, which leads to a decrease in the pK_a values of about 0.1. Ionic strength: 150 mM. Errors: pK_{a1} ± 0.2 and pK_{a1} ± 0.1.

Lowering amine basicity generally increases ligand bioavailability. This is also the case in this work, and some of the ligands [(±)-**2**, (±)-**3**, (±)-**27**, and (±)-**28**] indeed displayed moderate bioavailability and killed the parasite *P. falciparum* in cell-based assays with IC_{50} values around 2–7 μM.[19]

The question, which one of the two amine centers in the "diamine needle" (cf. Figure 1) is first being protonated, cannot be answered with confidence. Müller and coworkers[44] recently published a comprehensive review on how σ-inductive effects of substituents in the neighborhood of an amine center influence its basicity. Aryl sulfones were found to be among the most electron-withdrawing groups, strongly reducing amine basicity through σ transmission.

Taking into account incremental pK_a changes[44] (caused by σ induction from the aryl sulfone, the neighboring N center, and the aromatic S1/S3 substituent), pK_a values in the range of the experimental first pK_a value are calculated for *both* amine centers. Furthermore, at the active site of the aspartyl protease, the microenvironment of the two Asp side chains undoubtedly also affects the amine basicities in the needle.

However, it seems appropriate to assume that the bridging secondary amine of the azanorbornane is located between the two catalytically important aspartates and thereby in a preferred position to abstract a proton from a neighboring aspartate. This binding geometry is in full agreement with the modeling predictions.[22] The protonation of this amine is creating both an ion pair and a geometrically ideal H-bond network for both N–H protons. A protonated exocyclic amine would not be in a position to form *two* strong H bonds to the catalytic dyad. Therefore, it seems likely to assume the proton to sit on the cyclic amino function.

Conclusions and Outlook

The described compounds represent a family of aspartic protease inhibitors featuring a new needle to address the catalytic dyad of these enzymes. Guided by structure-based design, they have been decorated with binding elements that are complementary to the binding site of PM II. In vitro tests have shown that they also strongly inhibit the closely related, but still structurally not well characterized, malarial enzymes PM I and PM IV. This result is particularly important, as it has been shown that inhibition of all four related malarial proteases (PM I, PM II, HAP, and PM IV) is required to kill the parasite.[7,8] Our own, previously reported studies have demonstrated that these compounds are active against *P. falciparum* parasites in cell-based assays.[19] The aryl sulfone moiety is another key element in the ligands, by enforcing structural preorganization and by lowering the basicities of the amine centers in the *exo*-3-amino-7-azanorbornane needle, thereby enhancing ligand bioavailability.

The molecular recognition properties of the flap pocket were examined in greater detail, since its proper occupancy not only strengthens binding affinity but also increases the selectivity against the human aspartic proteases hCat D and E. The tolerance for ether O atoms within the flap pocket is strongly position-dependent. To reduce the lipophilicity of the flap-pocket vector and thus the amphiphilicity of the reported inhibitors, further studies with compounds comprising newly introduced heteroatoms are planned. Thereby, also the solubility of the compounds should be enhanced. Preliminary results already showed that fluorination of the compounds could be interesting. Also, a thioether scan of the flap-vector chain and the introduction of small aromatic (hetero)cycles are planned. To complement these studies, collaborative calculations are currently being performed to estimate better the entropic and enthalpic contributions to the enzyme–ligand binding processes of our compounds reported in this paper.

Experimental Section

Material and General Methods: 2-Naphthylmethylamine,[46] 4-hexylbenzylsulfonyl chloride,[47] 3-ethoxy-1-propyne[48] (**11p**), and 4-methoxy-1-butyne[49] (**11q**) were synthesized according to literature procedures. All reactions were carried out under N_2 or Ar; solvents and reagents were purchased from ABCR, Acros, Aldrich, or Fluka and used without further purification unless otherwise stated. Anhydrous (anh.) DMF (< 50 ppm H_2O) was purchased from Acros or Fluka. THF was freshly distilled from Na/benzophenone under N_2 before use. CH_2Cl_2 was distilled from CaH_2 and toluene from Na under N_2. Evaporation and concentration in vacuo were carried out by using a rotary evaporator with a bath temperature of 40 °C. Flash column chromatography was carried out by using SiO_2-60 (230–400 mesh, 0.040–0.063 mm, Fluka) at 25 °C with a head pressure of 0.0–0.4 bar and distilled technical solvents. In some cases, basic Al_2O_3, act. II (MP Alumina B, act. I, with addition of 3% wt. H_2O) was used (indicated in brackets where applicable, see the Supporting Information). All reported yields, unless otherwise specified, refer to chromatographically pure compounds. Thin-layer chromatography (TLC) was conducted on precoated SiO_2 glass plates F_{254} (Merck), silica gel plates ALUGRAM® SIL G/UV254 (0.20 mm silica gel 60 with fluorescence indicator UV254 on aluminum, Macherey–Nagel), or basic Al_2O_3 glass plates (TLC aluminum oxide 60 F_{254} basic, Merck). Visualization using UV light (254 nm) or by staining with a $KMnO_4$ solution (1.5 g of $KMnO_4$, 10 g of K_2CO_3, and 1.25 mL of 10% NaOH in 200 mL of H_2O). Medium-pressure liquid chromatography (MPLC) was conducted with a Büchi MPLC System with pump module C-601 & C-605 and fraction collector C-660 with a gradient by using the solvent mixtures indicated individually in parentheses. Melting points (M.p.) were measured with a Büchi B-540 melting-point apparatus in open capillaries and are uncorrected. Some compounds showed decomposition (decomp.) rather than a melting point. NMR spectra were measured with a Varian Gemini 300, a Varian Mercury 300, a Bruker ARX-300, or a Bruker AV-400 spectrometer at ambient temperature (unless otherwise noted). Apparent multiplicities are given in brackets. The residual solvent peak was used as the internal reference ($CDCl_3$: δ_H = 7.26 ppm, δ_C = 77.0 ppm. CD_3OD: δ_H = 4.84 ppm, δ_C = 49.05 ppm). H-1 to H-6 refer to the numbering of the bicyclic core as shown in Scheme 2; these arbitrary numbers for NMR assignment may differ from the locants used in the compound name. The 2D-NMR spectra were measured by the NMR Service, ETH Zürich. IR spectra: ATR-unit-upgraded (Golden Gate) Perkin–Elmer FT-IR Spectrum 1600 spectrometer (600–4000 cm^{-1}). When applicable, peak shape was characterized by br. (broad). High-resolution mass spectrometry (HRMS) was performed by the MS service of the Laboratorium for Organische Chemie, ETH Zürich. Matrix-assisted laser desorption ionization (MALDI): Varian IonSpec FT-ICR, 2,5-dihydroxybenzoic acid (DHB) or 3-hydroxypicolinic acid (3-HPA) as matrix; Electrospray ionization (ESI): Varian IonSpec FT-ICR, positive mode if not otherwise stated; Electron impact (EI): Waters Micromass AutoSpec-Ultima spectrometer. Elemental analyses were performed by the Mikrolabor of the Laboratorium for Organische Chemie, ETH Zürich. IUPAC names of the compounds were determined with the help of the program Name of Advanced Chemistry Development, Inc.[50]

In the following, the syntheses leading to inhibitor (±)-**14k** are described, also giving the experimental details.

1-Bromo-4-(ethynylsulfonyl)benzene (7): A mixture of 4-bromobenzenesulfonyl chloride (**5**; 16.38 g, 64.1 mmol) and $AlCl_3$ (8.55 g, 64.1 mmol) in CH_2Cl_2 (100 mL) was stirred at 25 °C under N_2 for

20 min. This solution was filtered and slowly added over 30 min to a cooled (0–5 °C) solution of bis(trimethylsilyl)acetylene (**6**; 13.0 mL, 58.3 mmol) in CH_2Cl_2 (50 mL). The cooling bath was removed, and the mixture was stirred at 25 °C for 18 h. The reaction was quenched by pouring into ice-cold 1 N HCl (300 mL), and the organic layer was separated, dried with Na_2SO_4, and concentrated to dryness in vacuo. Column chromatography (hexane/AcOEt, 4:1) simultaneously effected removal of the TMS protecting group to provide **7** as a brown solid (4.34 g, 30%). M.p. 60–62 °C. ^{1}H NMR (300 MHz, $CDCl_3$): δ = 3.61 (s, 1 H, HC≡), 7.72 (d, J = 8.7 Hz, 2 H, Ph), 7.84 (d, J = 8.7 Hz, 2 H, Ph) ppm. ^{13}C NMR (75 MHz, $CDCl_3$): δ = 80.0, 82.5, 129.4, 130.5, 133.1, 139.9 ppm. IR (neat): $\tilde{\nu}$ = 3228, 3086, 2059, 1920, 1571, 1471, 1393, 1333, 1285, 1184, 1156, 1084, 1067, 1012 cm^{-1}. HRMS (EI, 70 eV): calcd. for $C_8H_5BrO_2S^+$ [M$^+$] 243.9194; found 243.9193.

***tert*-Butyl (1*SR*,4*RS*)-2-[(4-Bromophenyl)sulfonyl]-7-azabicyclo[2.2.1]hepta-2,5-diene-7-carboxylate [(±)-8]:** A mixture of acetylene **7** (800 mg, 3.26 mmol) and *N*-Boc-pyrrole (1.09 mL, 6.53 mmol) was heated at 80 °C under N_2 for 18 h and with protection from light. The mixture was cooled to 25 °C and taken up in a minimum amount of CH_2Cl_2. Column chromatography (hexane/AcOEt, 3:1) yielded (±)-**8** as a beige solid (1.01 g, 75%). M.p. 120–125 °C. ^{1}H NMR (300 MHz, $CDCl_3$): δ = 1.28 [br. s, 9 H, $C(CH_3)_3$], 5.16 (s, 1 H, H-4), 5.40 (br. s, 1 H, H-1), 6.90 (dd, J = 2.7, 5.4 Hz, 1 H, H-5), 6.97 (br. s, 1 H, H-6), 7.65–7.75 (m, 5 H, H-3, Ph) ppm. ^{13}C NMR (75 MHz, $CDCl_3$): δ = 28.1, 67.1, 68.2, 81.7, 129.4, 129.7, 132.9, 138.2, 141.8, 143.5, 153.9 (2 C), 159.1 ppm. IR (neat): $\tilde{\nu}$ = 3094, 3017, 2976, 1699, 1571, 1476, 1455, 1387, 1349, 1314, 1278, 1256, 1149, 1117, 1084, 1066, 1018, 1006 cm^{-1}. HRMS (ESI): calcd. for $C_{17}H_{18}BrNNaO_4S^+$ [M + Na]$^+$ 434.0038; found 434.0032. $C_{17}H_{18}BrNO_4S$ (412.30): calcd. C 49.52, H 4.40, N 3.40; found C 49.55, H 4.59, N 3.37.

***tert*-Butyl (1*SR*,4*RS*)-2-[(4-Bromophenyl)sulfonyl]-7-azabicyclo[2.2.1]hept-2-ene-7-carboxylate [(±)-4]:** A suspension of $NaBH_4$ (413 mg, 10.9 mmol) in EtOH (15 mL) was added dropwise to a solution of $[Ni(OAc)_2(H_2O)_4]$ (2.72 g, 10.9 mmol) in EtOH (15 mL), and the resulting black slurry was stirred at 25 °C under N_2 for 10 min. A solution of diene (±)-**8** (900 mg, 2.18 mmol) in THF (9 mL) and 37% HCl (1.88 mL) was added, and stirring was continued for 16 h under N_2. The mixture was filtered through Celite and washed through with CH_2Cl_2 (50 mL). The filtrate was basified to pH 8 with saturated aqueous $NaHCO_3$ solution, and the organic layer was separated. The cloudy aqueous layer was further extracted with CH_2Cl_2 (2 × 20 mL), and the combined organics were dried with Na_2SO_4 and concentrated to dryness in vacuo to give (±)-**4** as a pale-brown solid that was used without further purification (900 mg, 100%). M.p. 128–130 °C. ^{1}H NMR (300 MHz, $CDCl_3$, 45 °C): δ = 1.24 [s, 9 H, $C(CH_3)_3$], 1.26–1.47 (m, 2 H, *endo*-H-5, *exo*-H-6), 1.91–2.10 (m, 2 H, *exo*-H-5, *endo*-H-6), 4.76 (d, J = 3.9 Hz, 1 H, H-1), 4.85 (br. s, 1 H, H-4), 7.13 (d, J = 2.1 Hz, 1 H, H-3), 7.71 (d, J = 8.7 Hz, 2 H, Ph), 7.80 (d, J = 8.7 Hz, 2 H, Ph) ppm. ^{13}C NMR (75 MHz, $CDCl_3$): δ = 24.3, 25.2, 28.1, 61.1, 62.1, 81.0, 129.3, 129.6, 132.9, 139.2, 145.1, 148.7, 154.8 ppm. IR (neat): $\tilde{\nu}$ = 2973 (br.), 1694, 1574, 1471, 1365, 1311, 1145, 1099, 1068, 1083, 1009 cm^{-1}. HRMS (ESI): calcd. for $C_{17}H_{20}BrNNaO_4S^+$ [M + Na]$^+$ 436.0194; found 436.0189. $C_{17}H_{20}BrNO_4S$ (414.31): calcd. C 49.28, H 4.87, N 3.38; found C 49.24, H 5.03, N 3.31.

***tert*-Butyl (1*SR*,2*SR*,3*RS*,4*RS*)-2-[(4-Bromophenyl)sulfonyl]-3-[(2-naphthylmethyl)amino]-7-azabicyclo[2.2.1]heptane-7-carboxylate [(±)-9c]:** Vinyl sulfone [(±)-**4**; 490 mg, 1.18 mmol] and 2-naphthylmethylamine (279 mg, 1.77 mmol) were dissolved in CH_2Cl_2 (3 mL) and concentrated to dryness in vacuo. The neat residue was heated at 90–100 °C under N_2 for 12 h. Column chromatography (CH_2Cl_2/AcOEt, 19:1) gave (±)-**9c** as a white solid (546 mg, 81%). A mixture of diastereoisomeric products was also isolated from the chromatographic purification (27 mg, 4%). These were not further purified or characterized. M.p. 127–139 °C. ^{1}H NMR (300 MHz, $CDCl_3$, 45 °C): δ = 1.43 [s, 9 H, $C(CH_3)_3$], 1.43–1.75 (m, 2 H, *endo*-H-5, *exo*-H-6), 1.87–1.98 (m, 1 H, *exo*-H-5), 2.36–2.44 (m, 1 H, *endo*-H-6), 3.26 (dt, J = 1.8, 4.5 Hz, 1 H, H-2), 3.31–3.32 (m, 1 H, H-3), 3.73 (d, J = 13.5 Hz, 1 H, NHCH_2), 3.92 (d, J = 13.5 Hz, 1 H, NHCH_2), 4.33 (d, J = 5.1 Hz, 1 H, H-4), 4.46 (t, J = 4.5 Hz, 1 H, H-1), 7.19 (d, J = 8.4 Hz, 1 H, napht.), 7.46–7.49 (m, 2 H, napht.), 7.57–7.68 (m, 5 H, Ph, napht.), 7.76–7.84 (m, 3 H, Ph, napht.) ppm. ^{13}C NMR (75 MHz, $CDCl_3$, 45 °C): δ = 24.6, 26.3, 28.4, 52.0, 57.8, 61.3, 64.5, 74.0, 80.9, 126.0, 126.4, 126.7, 126.8, 127.9, 128.0, 128.3, 129.3, 129.8, 132.8, 133.0, 133.6, 137.0, 139.5, 155.4 ppm. IR (neat): $\tilde{\nu}$ = 2974, 1698, 1574, 1509, 1471, 1389, 1364, 1309, 1275, 1249, 1144, 1098, 1083, 1067, 1009 cm^{-1}. HRMS (ESI): calcd. for $C_{28}H_{32}BrN_2O_4S^+$ [M + H]$^+$ 573.1242; found 573.1234. $C_{28}H_{31}BrN_2O_4S$ (571.53): calcd. C 58.84, H 5.47, N 4.90; found C 58.68, H 5.62, N 4.85.

***tert*-Butyl (1*SR*,2*SR*,3*RS*,4*RS*)-2-{[4-(3-Cyclopentylprop-1-yn-1-yl)-phenyl]sulfonyl}-3-[(2-naphthylmethyl)amino]-7-azabicyclo[2.2.1]-heptane-7-carboxylate [(±)-12k]:** A solution of (±)-**9c** (100 mg, 0.17 mmol) and 3-cyclopentylprop-1-yne (**11k**; 40 µL, 0.34 mmol) in $HNEt_2$ (3 mL) was prepared in a Schlenk tube under Ar and degassed with three freeze–pump–thaw cycles. $[PdCl_2(PPh_3)_2]$ (12 mg, 0.017 mmol) and CuI (6.7 mg, 0.035 mmol) were added to the solution at 25 °C. The black mixture was stirred at 55 °C for 13 h, then cooled to 25 °C, filtered over SiO_2 (AcOEt), and concentrated in vacuo. Purification of the residue by column chromatography (hexane/AcOEt, 17:3) yielded (±)-**12k** as an off-white solid (95 g, 93%). M.p. 126–128 °C. ^{1}H NMR (300 MHz, $CDCl_3$, 45 °C): δ = 1.28–1.77 (m, 8 H, CH_2 cyclopentyl), 1.43 [s, 9 H, $C(CH_3)_3$], 1.84–1.95 (m, 3 H, H-5, *exo*-H-6), 2.19 (hept., J = 7.5 Hz, 1 H, ≡CCH_2CH), 2.38–2.49 (m, 3 H, *endo*-H-6, ≡CCH_2), 3.27–3.40 (m, 2 H, H-2, H-3), 3.73 (d, J = 13.2 Hz, 1 H, NHCH_2), 3.90 (d, J = 13.2 Hz, 1 H, NHCH_2), 4.32 (d, J = 5.1 Hz, 1 H, H-4), 4.45 (t, J = 4.2 Hz, 1 H, H-1), 7.19 (d, J = 8.1 Hz, 1 H, napht.), 7.43–7.51 (m, 4 H, Ph, napht.), 7.57 (s, 1 H, napht.), 7.72–7.83 (m, 5 H, Ph, napht.) ppm. ^{13}C NMR (75 MHz, $CDCl_3$): δ = 24.6, 25.4, 25.4, 26.1, 28.3, 32.2, 39.0, 51.8, 57.6, 60.9, 64.2, 73.6, 79.4, 80.6, 95.1, 125.6, 125.9, 126.4 (2 C), 127.5, 127.7, 127.8, 127.9, 130.2, 132.2, 132.6, 133.2, 136.6, 138.1, 155.2 ppm. IR (neat): $\tilde{\nu}$ = 3008, 2936, 2869, 2226, 1702, 1592, 1467, 1367, 1323, 1294, 1272, 1254, 1160, 1143, 1132, 1100, 1084, 914, 876, 844, 816, 775, 759, 745, 662, 634, 622 cm^{-1}. HRMS (MALDI, 3-HPA): calcd. for $C_{36}H_{42}N_2O_4SNa^+$ [M + Na]$^+$ 599.2938; found 599.2948. $C_{36}H_{42}N_2O_4S$ (598.79): calcd. C 72.21, H 7.07, N 4.68; found C 72.08, H 7.01, N 4.59.

***tert*-Butyl (1*SR*,2*SR*,3*RS*,4*RS*)-2-{[4-(3-Cyclopentylpropyl)phenyl]-sulfonyl}-3-[(2-naphthylmethyl)amino]-7-azabicyclo[2.2.1]heptane-7-carboxylate [(±)-13k]:** Alkyne (±)-**12k** (44 mg, 0.073 mmol) and PtO_2 (4.4 mg, 10%) were combined in EtOH (4 mL) and stirred under a H_2 atmosphere (balloon) at 25 °C for 15 h. The mixture was filtered through Celite, concentrated in vacuo, and purified by column chromatography (CH_2Cl_2) to give (±)-**13k** as a white solid (40 mg, 91%). M.p. 98–100 °C. ^{1}H NMR (300 MHz, $CDCl_3$, 45 °C): δ = 0.99–1.12 (m, 2 H, cyclopentyl), 1.27–1.79 (m, 13 H, *endo*-5-H, *exo*-6-H, 11 aliph. H), 1.42 [s, 9 H, $C(CH_3)_3$], 1.82–1.95 (m, 1 H, *exo*-5-H), 2.41–2.49 (m, 1 H, *endo*-6-H), 2.68 (t, J = 7.8 Hz, 2 H, Ar–CH_2), 3.32 (dt, J = 1.5, 4.5 Hz, 1 H, 2-H), 3.37–3.38 (m, 1 H, 3-H), 3.73 (d, J = 13.2 Hz, 1 H, NHCH_2), 3.89 (d, J = 13.2 Hz, 1 H, NHCH_2), 4.30 (d, J = 5.1 Hz, 1 H, 4-H), 4.41 (t, J = 4.5 Hz, 1 H, 1-H), 7.23 (d, J = 8.1 Hz, 1 H, napht.), 7.31 (d, J

= 8.4 Hz, 2 H, Ph), 7.42–7.49 (m, 2 H, napht.), 7.60 (s, 1 H, napht.), 7.73–7.82 (m, 5 H, Ph, napht.) ppm. ^{13}C NMR (75 MHz, $CDCl_3$): δ = 24.4, 25.2, 26.1, 28.3, 30.3, 32.7, 35.8, 36.3, 40.0, 51.8, 57.6, 61.3, 64.2, 73.4, 80.5, 125.6, 125.9, 126.4, 127.5, 127.6, 127.9, 128.0 (2 C), 129.2, 132.5, 133.2, 136.7, 137.0, 149.6, 155.2 ppm. IR (neat): $\tilde{\nu}$ = 2935, 2861, 1689, 1595, 1458, 1380, 1366, 1299, 1248, 1163, 1147, 1118, 1084, 1053, 901, 879, 854, 827, 809, 783, 768, 755, 686, 656, 634 cm^{-1}. HRMS (MALDI, 3-HPA): calcd. for $C_{36}H_{47}N_2O_4S^+$ $[M + H]^+$ 603.3251; found 603.3241. $C_{36}H_{46}N_2O_4S$ (602.83): calcd. C 71.73, H 7.69, N 4.65; found C 71.93, H 7.74, N 4.58.

(1*RS*,2*RS*,3*RS*,4*SR*)-3-{[4-(3-Cyclopentylpropyl)phenyl]sulfonyl}-*N*-(2-naphthylmethyl)-7-azabicyclo[2.2.1]heptan-2-amine Bis(hydrobromide) [(±)-14k]: Carbamate (±)-**13k** (20 mg, 0.033 mmol) was dissolved in CH_2Cl_2 (2 mL) under Ar and cooled to –78 °C. A solution of BBr_3 (1 M in CH_2Cl_2, 200 µL) was added in a dropwise manner. After stirring at –78 °C for 15 min, MeOH (2 mL) was added to quench the reaction, and the solution was warmed up to 25 °C. MeOH (2 mL) was added, and the solution was concentrated in vacuo (3×) to give (±)-**14k** as an off-white solid (22 mg, 100%). M.p. 110–115 °C (decomp.). ^{1}H NMR (300 MHz, CD_3OD): δ = 0.85–0.89 (m, 2 H, cyclopentyl), 1.19–1.56 (m, 11 H, *endo*-5-H, *exo*-6-H, 9 aliph. H), 1.94–2.12 (m, 2 H, aliph. H), 2.22–2.33 (m, 1 H, *exo*-5-H), 2.71 (t, *J* = 7.8 Hz, 2 H, Ar–CH_2), 2.78–2.86 (m, 1 H, *endo*-6-H), 4.02 (d, *J* = 12.3 Hz, 1 H, NHCH_2), 4.17 (d, *J* = 12.3 Hz, 1 H, NHCH_2), 4.50 (d, *J* = 4.5 Hz, 1 H, 2-H), 4.53–4.56 (m, 1 H, 3-H), 4.79 (d, *J* = 5.4 Hz, 1 H, 4-H), 5.20–5.23 (m, 1 H, 1-H), 7.53–7.67 (m, 5 H, Ph, napht.), 7.87–7.91 (m, 2 H, napht.), 7.93 (s, 1 H, napht.), 8.05–8.08 (m, 3 H, Ph, napht.) ppm. ^{13}C NMR (75 MHz, CD_3OD): δ = 22.6, 24.9, 25.7, 31.4, 33.3, 36.5, 36.9, 40.9, 51.5, 61.1, 61.4, 64.3, 66.6, 127.4, 127.8, 128.4, 128.8, 128.9, 129.6 (2 C), 129.7, 130.8, 131.0, 134.1, 134.6, 135.6, 153.0 ppm. IR (neat): $\tilde{\nu}$ = 3386 (br.), 2932, 2856, 2656, 2512, 1594, 1450, 1313, 1273, 1147, 1086, 1017, 856, 816, 744, 685, 659 cm^{-1}. HRMS (MALDI, 3-HPA): calcd. for $C_{31}H_{39}N_2O_2S^+$ $[M - HBr_2]^+$ 503.2727; found 503.2734.

Crystals of (±)-9b: Grown by vapor diffusion of pentane into AcOEt; colorless cube, 0.24 × 0.24 × 0.16 mm; monoclinic $P2_1/c$; a = 9.859(1) Å, b = 26.741(1) Å, c = 10.01(1) Å, β = 96.89(1)°, V = 2641 Å^3; D_x = 1.314 mg m^{-3}; $2\theta_{max}$ = 55.70°; Mo-K_α radiation, λ = 0.71073 Å; T = 172 K; 5900 independent of 8339 measured reflections R_{int} = 0.036, no absorption correction applied (μ = 0.165 mm^{-1}); structure solution using SIR97;[51] 4387 reflections with $I > 2\sigma(I)$ refined on $|F^2|$ using SHELXL-97;[52] Δ/σ_{max} = 4.201, $\Delta\rho_{max}$ = 0.392 e Å^{-3}, $\Delta\rho_{min}$ = –0.530 e Å^{-3}; 470 parameters, all H atom parameters refined; R(all) = 0.0820, R(gt) = 0.0548, wR(ref) = 0.1797, wR(gt) = 0.1485.

Crystals of (±)-13f: Grown by slow evaporation from MeOH/hexane solution; colorless cube, 0.3 × 0.16 × 0.02 mm; monoclinic $P2_1/n$; a = 10.900(1) Å, b = 9.835(1) Å, c = 30.400(2) Å, β = 92.13(1)°, V = 3257 Å^3; D_x = 1.205 mg m^{-3}; $2\theta_{max}$ = 23.03°; Mo-K_α radiation, λ = 0.71073 Å; T = 223 K; 4397 independent of 13637 measured reflections R_{int} = 0.065, no absorption correction applied (μ = 0.139 mm^{-1}); structure solution using SIR97;[51] 3011 reflections with $I > 2\sigma(I)$ refined on $|F^2|$ using SHELXL-97;[52] Δ/σ_{max} = 0.033, $\Delta\rho_{max}$ = 0.493 e Å^{-3}, $\Delta\rho_{min}$ = –0.341 e Å^{-3}; 377 parameters, all H atom positions constrained; R(all) = 0.2215, R(gt) = 0.1663, wR(ref) = 0.3405, wR(gt) = 0.3209. Heavily disordered naphthyl and *n*-heptane fragment cause bad agreement factor.

CCDC-711327 [for (±)-**9b**] and -711328 [for (±)-**13f**] contain the supplementary crystallographic data for this paper. These data can be obtained free of charge from The Cambridge Crystallographic Data Centre via www.ccdc.cam.ac.uk/data_request/cif.

Supporting Information (see footnote on the first page of this article): Synthetic protocols and characterization data of the reported compounds; ORTEP figure of (±)-**13f**; information on modeling; short description of the assay of in vitro enzyme activity.

Acknowledgments

We gratefully acknowledge financial support from the Novartis Foundation (F. H.), the Human Frontier Science Program (F. H.), the ETH Research Council, and the Roche Research Foundation (PhD fellowship to M. Z.). We thank Christoph Fäh and Pascal Wyss for synthetic contributions and Jun Liu and Prof. Daniel E. Goldberg for determination of some IC_{50} values. The pK_a values were determined by Dr. Björn Wagner, F. Hoffmann-La Roche Ltd, Basel. We thank Dr. Carlo Thilgen for help with the nomenclature.

[1] R. W. Snow, C. A. Guerra, A. M. Noor, H. Y. Myint, S. I. Hay, *Nature* **2005**, *434*, 214–217.
[2] C. H. Sibley, J. E. Hyde, P. F. G. Sims, C. V. Plowe, J. G. Kublin, E. K. Mberu, A. F. Cowman, P. A. Winstanley, W. M. Watkins, A. M. Nzila, *Trends Parasitol.* **2001**, *17*, 582–588.
[3] A. M. Silva, A. Y. Lee, S. V. Gulnik, P. Majer, J. Collins, T. N. Bhat, P. J. Collins, R. E. Cachau, K. E. Luker, I. Y. Gluzman, S. E. Francis, A. Oksman, D. E. Goldberg, J. W. Erickson, *Proc. Natl. Acad. Sci. USA* **1996**, *93*, 10034–10039.
[4] S. E. Francis, D. J. Sullivan Jr., D. E. Goldberg, *Annu. Rev. Microbiol.* **1997**, *51*, 97–123.
[5] R. Banerjee, J. Liu, W. Beatty, L. Pelosof, M. Klemba, D. E. Goldberg, *Proc. Natl. Acad. Sci. USA* **2002**, *99*, 990–995.
[6] A. Nezami, I. Luque, T. Kimura, Y. Kiso, E. Freire, *Biochemistry* **2002**, *41*, 2273–2280.
[7] J. Liu, I. Y. Gluzman, M. E. Drew, D. E. Goldberg, *J. Biol. Chem.* **2005**, *280*, 1432–1437.
[8] A. L. Omara-Opyene, P. A. Moura, C. R. Sulsona, J. A. Bonilla, C. A. Yowell, H. Fujioka, D. A. Fidock, J. B. Dame, *J. Biol. Chem.* **2004**, *279*, 54088–54096.
[9] J. Liu, E. S. Istvan, I. Y. Gluzman, J. Gross, D. E. Goldberg, *Proc. Natl. Acad. Sci. USA* **2006**, *103*, 8840–8845.
[10] J. A. Bonilla, P. A. Moura, T. D. Bonilla, C. A. Yowell, D. A. Fidock, J. B. Dame, *Int. J. Parasitol.* **2007**, *37*, 317–327.
[11] J. A. Bonilla, T. D. Bonilla, C. A. Yowell, H. Fujioka, J. B. Dame, *Mol. Microbiol.* **2007**, *65*, 64–75.
[12] M. E. Drew, R. Banerjee, E. W. Uffman, S. Gilbertson, P. J. Rosenthal, D. E. Goldberg, *J. Biol. Chem.* **2008**, *283*, 12870–12876.
[13] O. A. Asojo, E. Afonina, S. V. Gulnik, B. Yu, J. W. Erickson, R. Randad, D. Medjahed, A. M. Silva, *Acta Crystallogr., Sect. D: Biol. Crystallogr.* **2002**, *58*, 2001–2008.
[14] L. Prade, A. F. Jones, C. Boss, S. Richard-Bildstein, S. Meyer, C. Binkert, D. Bur, *J. Biol. Chem.* **2005**, *280*, 23837–23843.
[15] C. Boss, O. Corminboeuf, C. Grisostomi, S. Meyer, A. F. Jones, L. Prade, C. Binkert, W. Fischli, T. Weller, D. Bur, *ChemMedChem* **2006**, *1*, 1341–1345.
[16] D. A. Carcache, S. R. Hörtner, A. Bertogg, C. Binkert, D. Bur, H. P. Märki, A. Dorn, F. Diederich, *ChemBioChem* **2002**, *3*, 1137–1141.
[17] D. A. Carcache, S. R. Hörtner, A. Bertogg, F. Diederich, A. Dorn, H. P. Märki, C. Binkert, D. Bur, *Helv. Chim. Acta* **2003**, *86*, 2192–2209.
[18] D. A. Carcache, S. R. Hörtner, P. Seiler, F. Diederich, A. Dorn, H. P. Märki, C. Binkert, D. Bur, *Helv. Chim. Acta* **2003**, *86*, 2173–2191.
[19] F. Hof, A. Schütz, C. Fäh, S. Meyer, D. Bur, J. Liu, D. E. Goldberg, F. Diederich, *Angew. Chem.* **2006**, *118*, 2193–2196; *Angew. Chem. Int. Ed.* **2006**, *45*, 2138–2141.
[20] J. Yuvaniyama, A. D'Arcy, C. Oefner, H. Lötscher, D. Bur, G. E. Dale, H. P. Märki, F. K. Winkler, R. P. Moon, R. G. Rid-

ley in *Symposium on Parasite Proteases as Drug Targets*, University of Glasgow, UK, **2000**.

[21] R. Rajamani, C. H. Reynolds, *J. Med. Chem.* **2004**, *47*, 5159–5166.

[22] P. R. Gerber, K. Müller, *J. Comput.-Aided Mol. Des.* **1995**, *9*, 251–268.

[23] *Spartan 06*, Wavefunction, Inc., Irvine, USA, **2006**. The DFT-B3LYP (6-31G* basis set, MP2 correlation) calculations as implemented by the software were used.

[24] The Cambridge Structural Database: a quarter of a million crystal structures and rising. F. H. Allen, *Acta Crystallogr., Sect. B: Struct. Sci.* **2002**, *58*, 380–388. CSD search: CSD version 5.29, November 2007, inclusive updates January 2008, containing about 440000 entries. All searches were performed for structures with R factor ≤ 0.1 (not disordered, no error), excluding polymeric, powder, or organometallic compounds.

[25] A. K. H. Hirsch, S. Lauw, P. Gersbach, W. B. Schweizer, F. Rohdich, W. Eisenreich, A. Bacher, F. Diederich, *ChemMedChem* **2007**, *2*, 806–810.

[26] D. A. Bors, A. Streitwieser Jr., *J. Am. Chem. Soc.* **1986**, *108*, 1397–1404.

[27] Z. Chen, M. L. Trudell, *Synth. Commun.* **1994**, *24*, 3149–3155.

[28] F. Liang, H. A. Navarro, P. Abraham, P. Kotian, Y.-S. Ding, J. Fowler, N. Volkow, M. J. Kuhar, F. I. Carroll, *J. Med. Chem.* **1997**, *40*, 2293–2295.

[29] R. Leung-Toung, Y. Liu, J. M. Muchowski, Y.-L. Wu, *J. Org. Chem.* **1998**, *63*, 3235–3250.

[30] D. M. Hodgson, C. R. Maxwell, R. Wisedale, I. R. Matthews, K. J. Carpenter, A. H. Dickenson, S. Wonnacott, *J. Chem. Soc. Perkin Trans. 1* **2001**, 3150–3158.

[31] J. P. Wolfe, R. A. Singer, B. H. Yang, S. L. Buchwald, *J. Am. Chem. Soc.* **1999**, *121*, 9550–9561.

[32] V. Voorhees, R. Adams, *J. Am. Chem. Soc.* **1922**, *44*, 1397–1405.

[33] M. Sakaitani, Y. Ohfune, *J. Org. Chem.* **1990**, *55*, 870–876.

[34] A. H. Fauq in *Encyclopedia of Reagents for Organic Synthesis* (Ed.: L. Paquette), Wiley & Sons, New York, **2004**.

[35] M. Zürcher, T. Gottschalk, S. Meyer, D. Bur, F. Diederich, *ChemMedChem* **2008**, *3*, 237–240.

[36] K. E. Luker, S. E. Francis, I. Y. Gluzman, D. E. Goldberg, *Mol. Biochem. Parasitol.* **1996**, *79*, 71–78.

[37] C. Boss, S. Richard-Bildstein, T. Weller, W. Fischli, S. Meyer, C. Binkert, *Curr. Med. Chem.* **2003**, *10*, 883–907.

[38] PM3–Monte Carlo; *Spartan 06*, Wavefunction, Inc., Irvine, USA, **2006**.

[39] Log D values were calculated by using the program Log D, version 11.0, Advanced Chemistry Development, Inc., Toronto ON, Canada, www.acdlabs.com, **2006**.

[40] J. A. Olsen, D. W. Banner, P. Seiler, U. Obst Sander, A. D'Arcy, M. Stihle, K. Müller, F. Diederich, *Angew. Chem.* **2003**, *115*, 2611–2615; *Angew. Chem. Int. Ed.* **2003**, *42*, 2507–2511.

[41] K. Müller, C. Faeh, F. Diederich, *Science* **2007**, *317*, 1881–1886.

[42] V. S. Bryantsev, M. S. Diallo, W. A. Goddard, *J. Phys. Chem. A* **2007**, *111*, 4422–4430.

[43] M. R. Crampton, I. A. Robotham, *J. Chem. Res.* **1997**, 22–23.

[44] M. Morgenthaler, E. Schweizer, A. Hoffmann-Röder, F. Benini, R. E. Martin, G. Jaeschke, B. Wagner, H. Fischer, S. Bendels, D. Zimmerli, J. Schneider, F. Diederich, M. Kansy, K. Müller, *ChemMedChem* **2007**, *2*, 1100–1115.

[45] R. R. Fraser, R. B. Swingle, *Can. J. Chem.* **1970**, *48*, 2065–2074.

[46] W. L. Cody, D. D. Holsworth, N. A. Powell, M. Jalaie, E. Zhang, W. Wang, B. Samas, J. Bryant, R. Ostroski, M. J. Ryan, J. J. Edmunds, *Bioorg. Med. Chem.* **2005**, *13*, 59–68.

[47] T. Yamaguchi, T. Seki, T. Tamaki, K. Ichimura, *Bull. Chem. Soc. Jpn.* **1992**, *65*, 649–656.

[48] L. Brandsma in *Studies in Organic Chemistry*, Elsevier Science, Amsterdam, **1988**, vol. 34, p. 259ff.

[49] K. F. Shaw, A. J. Welch, *Polyhedron* **1992**, *11*, 157–167.

[50] Name, 8.00 release, product version 8.17, Advanced Chemistry Development, Inc., Toronto ON, Canada, www.acdlabs.com, **2005**.

[51] A. Altomare, M. C. Burla, M. Camalli, G. L. Cascarano, C. Giacovazzo, A. Guagliardi, A. G. G. Moliterni, G. Polidori, R. Spagna, *J. Appl. Crystallogr.* **1999**, *32*, 115–119.

[52] Sheldrick, G. M., *SHELXL97: Program for the Refinement of Crystal Structures*, University of Göttingen, Göttingen, Germany, **1997**.

Received: November 28, 2008
Published Online: March 5, 2009

